

# Preliminary study on a kinetic energy recovery system for sailing yachts

Giuseppe Leo Guizzi<sup>a</sup>, Michele Manno<sup>a,\*</sup>, Guido Manzi<sup>b</sup>, Marco Salvatori<sup>a</sup>,  
Domenico Serpella<sup>b</sup>

<sup>a</sup>*Dept. of Industrial Engineering, University of Rome Tor Vergata, Italy*

<sup>b</sup>*Labor srl, Tecnopolo Tiburtino, Via G. Peroni 386, 00131 Rome, Italy*

---

## Abstract

This paper presents the preliminary theoretical results obtained on a model of a kinetic energy recovery system for sailing yachts, based on the conversion of wave-induced boat oscillations (heave, pitch and roll) into electric energy by means of a linear generator.

The recovery system is based on a linear generator, with a mass oscillating along the vertical axis and gaining kinetic energy: the resulting mechanical energy can be extracted (by means of electromagnetic damping) and converted into electricity. The oscillating mass incorporates permanent magnets which, moving in proximity of stator windings, generate electric power due to electromagnetic induction.

The device aims at recovering as much kinetic energy as possible from the natural movements of a sailing yacht on the sea, therefore taking the view of a boat as a moving wave energy converter with energy harvesting capability. The boat's motions can be vertical oscillations due to the buoyancy in the presence of sea waves, both when the boat is still or sailing, and rolling and pitching motions originated both by sailing in wavy waters and by the normal boat dynamics due to the sails' propulsion. Linear generators will convert kinetic energy into electrical energy to be used as "green" electricity for any possible application on board.

---

\*Corresponding author

*Email addresses:* guizzi@ing.uniroma2.it (Giuseppe Leo Guizzi),  
michele.manno@uniroma2.it (Michele Manno), g.manzi@labor-roma.it (Guido Manzi), marco.salvatori87@gmail.com (Marco Salvatori),  
d.serpella@labor-roma.it (Domenico Serpella)

Preliminary calculations show that a properly configured system could be able to recover approximately 100 W under most sea conditions on an almost continuous basis, which can be an extremely attractive result since an electric energy availability of 1-2 kWh on a sailing yacht is of significant interest.

*Keywords:* Wave Energy Recovery, Linear Generator, Sail Yacht, Kinetic Energy Recovery System, SEAKERS

---

## 1. Introduction

This paper presents the preliminary theoretical results obtained on a model of a kinetic energy recovery system to be used on board of sail yachts in order to recover energy from the wave-induced boat's vertical motion (SEAKERS: SEA Kinetic Energy Recovery System).

Such a system would be able to recover actual free energy, as opposed to other devices, already commercially available, that subtracts energy from the propulsion offered by the wind's lift on the sails, as in the case of micro-wind turbines installed on the boat, which are set into motion by the apparent wind originating from the yacht's motion.

This system could address a well known unsatisfied requirement of yacht owners, since energy is a resource of primary importance in a boat, especially in a sailing one: it is well known that during a one-day cruise, electricity consumption has to be carefully managed (for instance the refrigerator is switched off), so as not to be short of energy at night. It often happens that, after one day of sail cruise, it is necessary to recharge the batteries through the on-board generator, which means keeping it on for hours, producing very annoying noise, smoke and pollution.

In practical terms, the SEAKERS device is intended to be a linear oscillator, with a mass oscillating along the vertical axis and gaining kinetic energy; if the mass is the moving element of a linear generator, the resulting mechanical energy can be extracted and converted into electricity. The oscillating mass incorporates permanent magnets which, moving in proximity of stator windings, generate electric power due to electromagnetic induction.

Basically, two emerging fields represent the conceptual background for this work: wave energy conversion, with particular reference to single-body heaving buoys with linear wave energy converters [1–6], and energy harvesting from ambient vibration [7, 8].

29 In particular, the idea of using a linear generator originates from work  
30 carried out at the University of Uppsala [9–13], where such devices have been  
31 designed and tested in order to recover wave energy from a buoy, oscillating  
32 on the sea surface, connected to a rope that makes a piston move inside a  
33 generator placed on the sea floor. In the SEAKERS project, the oscillating  
34 mass is set into motion not directly by the sea waves but by its inertia as the  
35 yacht is subject to heave, pitch and roll motions: in this respect the system  
36 acts like an energy harvester, even though on a bigger scale if compared to  
37 the generators usually taken into consideration in this field, which usually  
38 provide electric power of tens or thousandths of microwatts [14].

39 In order to design and prototype the generator, it is necessary to set up  
40 a reliable model of different sea conditions that could be of practical interest  
41 for a normal cruise on a sail yacht (thus there is no need to consider extreme,  
42 stormy waves) and of the ship motion due to such sea states. Furthermore, it  
43 is important to find out, by means of a linearised model of the generator, how  
44 much power could be extracted for different operating conditions, in order  
45 to decide whether the project’s outcome could be in principle commercially  
46 viable, and quickly to provide data against which results from more detailed  
47 analytical models and experimental tests could later be compared.

48 This paper presents the preliminary analysis carried out in the first stage  
49 of the project, describing the assumptions and the details of the mathematical  
50 model regarding wave excitation, yacht’s response, and power generation by  
51 the linear oscillator (section 2), and the results of simulations (section 3).

## 52 2. Mathematical model

### 53 2.1. Wave spectra

54 The main characteristic of sea waves is randomness. Indeed, by checking  
55 even a short time series, two characteristics arise: height and period of a  
56 wave are different from height and period of another wave. For this reason,  
57 the free surface elevation of sea waves is modelled as a stochastic process and  
58 is assumed to be a random, Gaussian, ergodic process in the time domain  
59 [15–18]; mathematically, the physical properties of sea waves are conveyed  
60 by the one-sided spectral density  $S_{\zeta}(\omega)$  [17], where  $\omega$  is the wave frequency<sup>1</sup>,

---

<sup>1</sup>In this paper, the term “frequency” will be used indifferently to identify both frequency  $f$ , measured in Hz, or angular (circular) frequency  $\omega$ , measured in rad/s.

61 which is related to the wave number by the dispersion relation, which, in  
62 deep water is [15–18]:

$$\omega^2 = kg \quad (1)$$

63 where  $g$  is the acceleration of gravity. (It may be useful to recall that wave  
64 number and wave length are mutually dependent:  $k = 2\pi/\lambda$ ).

65 The spectral density is correlated to the overall energy content of the sea  
66 state, therefore, statistical data that can be gleaned from the spectral density  
67 correspond to important parameters for the description of a sea state. Of  
68 particular importance is the 0-th spectrum moment  $m_0$ , which is equivalent  
69 to the area under the wave spectrum curve, because many relevant physical  
70 properties directly derive from it. In particular, one of the most useful pa-  
71 rameter to represent the sea state is the significant wave height, which is the  
72 average wave height (crest to trough) of the one-third largest waves, and for  
73 narrow band spectra it is given by [15–18]:

$$h_s = 4\sqrt{m_0} \quad (2)$$

74 The simulations that will be presented in the following sections were  
75 carried out taking into account statistical wave data for the Mediterranean  
76 Sea, with particular reference to measurements taken at Capo Linaro (Civi-  
77 tavecchia, Italy) by ISPRA (Istituto Superiore per la Protezione e la Ricerca  
78 Ambientale) from January 2<sup>nd</sup>, 2004, to September 12<sup>th</sup>, 2006.

79 In the case of random waves, it is possible to find a particular set of  
80 parameters that make the JONSWAP spectrum suitable to represent sea  
81 conditions in the location of interest.

82 The JONSWAP spectrum was developed from extensive field measure-  
83 ments in the context of the Joint North Sea Wave Project [15–18]. This  
84 formulation is suitable for wind-generated waves in fetch limited locations.  
85 The inputs are the wind speed and the fetch length. The mathematical  
86 formulation is given by the following equation:

$$S_\zeta(\omega) = \alpha g^2 \omega_p^{-5} \exp \left[ -\frac{5}{4} \left( \frac{\omega}{\omega_p} \right)^{-4} \right] \exp \left\{ \log \gamma \exp \left[ -\frac{(\omega - \omega_p)^2}{2\sigma^2 \omega_p^2} \right] \right\} \quad (3)$$

87 In the above equation,  $\omega_p = 2\pi/T_p$  is the peak circular frequency,  $\alpha$  is  
88 the Phillips' parameter given by  $\alpha = 0.0076(gx/\bar{U})^{-0.22}$ , where  $x$  is the fetch  
89 length and  $\bar{U}$  the mean wind speed, and  $\gamma$  is the peak-shape parameter. For

90 practical applications,  $\sigma$  can be assumed equal to 0.08 in the whole frequency  
91 domain.

92 Sea conditions at the chosen location are well represented by a bimodal  
93 spectrum [19, 20], with the relationship between peak period and significant  
94 wave height governed by two parameters ( $\alpha$  and  $\gamma$ ):

$$T_p = f(\alpha, \gamma) \sqrt{h_s/g} \quad (4)$$

95 The bimodal JONSWAP spectrum is completely defined when the signifi-  
96 cant wave height  $h_s$  and parameters  $\alpha$  and  $\gamma$ , along with the function  $f(\alpha, \gamma)$ ,  
97 are specified.

98 In order to represent correctly sea conditions at Capo Linaro, values of  
99  $\alpha$ ,  $\gamma$ ,  $f(\alpha, \gamma)$  and  $T_p$  are chosen according to table 1 (F. Arena, personal  
100 communications, 2012). The corresponding wave spectra are illustrated in  
101 fig. 1.

## 102 2.2. Yacht model

### 103 2.2.1. Encounter frequency

104 Due to its forward speed  $V$ , the wave spectrum for the ship is different  
105 than for a fixed observer. When studying the ship's response it is therefore  
106 necessary to take into account the frequency at which it actually encounters  
107 the waves (*encounter frequency*). The encounter frequency depends on wave  
108 velocity, ship speed and heading, i.e. the relative direction of the ship with  
109 respect to waves. Headings are denoted by means of the angle  $\mu$ , which is  
110 defined between the forward directions of wave and ship: thus for bow waves  
111  $\mu = \pi$ , for transverse waves  $\mu = \pi/2$ , and for aft waves  $\mu = 0$ .

112 For seakeeping purposes, the assumption of deep water may be applied; in  
113 this case, taking into account the dispersion relation, eq. (1), the encounter  
114 frequency  $\omega_e$  can be derived as:

$$\omega_e = \omega - \frac{\omega^2 V}{g} \cos \mu \quad (5)$$

115 The spectral density must be modified according to the encounter fre-  
116 quency (it is practically a Doppler shift of the spectrum). Since the energy  
117 content of a spectrum must be the same for any observer, fixed or moving  
118 with the ship, the 0-th momentum must be the same; as a result, the spectral

119 density  $S_{\zeta_e}$  experienced by the ship is given by [18]:

$$S_{\zeta_e}(\omega_e) = \frac{S_{\zeta}(\omega)}{\left|1 - 2\frac{\omega V}{g} \cos \mu\right|} \quad (6)$$

### 120 2.2.2. Response amplitude operators

121 The frame of reference on a ship usually consists of a  $X$ -axis that coincides  
122 with the longitudinal axis of the ship and points from aft to bow, of a  $Y$ -axis  
123 that coincides with the transverse axis and points from port to starboard,  
124 and finally of a  $Z$ -axis for the vertical direction (positive upwards).

125 The six degrees of freedom for a ship are heave (vertical motion on the  
126  $Z$ -axis), surge (longitudinal motion on the  $X$ -axis), sway (lateral motion on  
127 the  $Y$ -axis), yaw (oscillation around the vertical  $Z$ -axis), pitch (oscillation  
128 around the transverse  $Y$ -axis), roll (oscillation around the longitudinal  $X$ -  
129 axis). In this paper, only heave, pitch and roll are of interest, and they will  
130 be denoted respectively by variables  $z$ ,  $\vartheta$  and  $\eta$ .

131 The ship response to the wave excitation is usually described in terms  
132 of transfer functions (RAO, Response Amplitude Operator) [15–18], which  
133 give the normalised amplitude of the resulting ship's motion for a sinusoidal  
134 excitation of frequency  $\omega_e$ , the normalization factor being the wave amplitude  
135  $\zeta_0$  for linear motions and the wave slope  $k\zeta_0 = 2\pi\zeta_0/\lambda$  for angular motions.

$$\text{RAO}_z(\omega_e) = z_0/\zeta_0 \quad (7)$$

136

$$\text{RAO}_{\vartheta}(\omega_e) = \vartheta_0/k\zeta_0 \quad (8)$$

137 Obviously, equally important are the phase shifts  $\varphi$  of each motion with  
138 respect to the wave excitation. With the knowledge of RAOs and phase shifts,  
139 it is possible to reconstruct heave, pitch and roll motions from a sinusoidal  
140 wave excitation. Therefore, based on the chosen frame of reference described  
141 at the beginning of this section, and taking into account that angular motions  
142 (pitch and roll) are usually small, vertical oscillations for any point on the  
143 ship may be calculated as follows:

$$y(t) \cong z(t) - L\vartheta(t) + B\vartheta(t) \quad (9)$$

144 where  $L$  and  $B$  are the longitudinal and lateral distance of any point on the  
145 ship from the center of gravity.

146 Therefore, being the sum of harmonic motions (phasors), the vertical  
147 oscillation  $y$  is also represented by a harmonic oscillation, and it is possible  
148 to define a RAO for the particular point of interest on the ship:

$$\text{RAO}_y(\omega_e) = y_0/\zeta_0 \quad (10)$$

149 In case of a random wave excitation, with the assumption that the re-  
150 sponse is a linear function of wave amplitude and applying the superposition  
151 principle, vertical motion can be reconstructed as:

$$y(t) = \sum_{j=1}^n y_{0,j} \cos(\omega_{e,j}t + \varphi_{y,j}) \quad (11)$$

152 where each oscillation amplitude  $y_{0,j}$  is a function of frequency and amplitude  
153 of the  $j$ -th harmonic, according to eq. (10).

154 Furthermore, it is possible to demonstrate that the ship's response spec-  
155 tral density is given by the product of the square of the RAO and the wave  
156 spectral density. Thus, for any point on the ship the spectral density associ-  
157 ated to its wave-induced motion is:

$$S_y(\omega_e) = \text{RAO}_y^2(\omega_e)S_{\zeta_e}(\omega_e) \quad (12)$$

### 158 2.3. Linear generator

#### 159 2.3.1. Equation of motion

160 The linear generator used to recover energy from the wave-induced mo-  
161 tions of the yacht is analysed and approximated in this paper as a simple  
162 linear mechanical oscillator [7], where the damping element represents a linear  
163 approximation of the effect of the electromagnetic force exerted by the gen-  
164 erator as it provides a voltage difference proportional to the time derivative  
165 of the magnetic flux, and the spring represents the stiffness of the generator's  
166 support. It is assumed that the damping coefficient can be dynamically var-  
167 ied depending on sea conditions: this could be achieved in the final system  
168 by means of power electronics. Indeed, as the following sections will show  
169 clearly, it is very important to control the damping coefficient in order to  
170 achieve the best performance in terms of power generation under different  
171 operating conditions [10].

172 It is further assumed that the support can exert such a static force in order  
173 to balance the weight of the oscillating mass; it can be seen that mechanical  
174 springs cannot play such a role, because the resulting stiffness would be too

175 high for the typical forcing frequencies. For example, if the spring were to  
176 counterbalance the weight with a limited elongation at rest  $l = 0.05$  m, the  
177 resulting natural frequency would be  $\omega_n = \sqrt{g/l} \cong 2.2$  Hz, which is much  
178 larger than the forcing frequency of sea waves: this would make the system  
179 too stiff, i.e. the mass would move rigidly with the basement, with no relative  
180 motion between the two and, thus, no power extracted.

181 In the prototype that is being subjected to its first experimental testing,  
182 weight is balanced by the static forces generated by the interaction of coils  
183 and permanent magnets, placed in the moving part of the generator, with  
184 the “stator”, which is simply an iron cylinder lathed with teeth and cavities  
185 (fig. 2). Other strategies could have been chosen to balance the weight of the  
186 oscillating mass, such as a pneumatic system: in this case, a proper selection  
187 of volumes could result in the desired (low) stiffness. However, the specific  
188 mechanism is not of particular interest for the analysis carried out in this  
189 paper, and in what follows it is simply assumed that static forces (weight  
190 and support) cancel each other.

191 The equation of motion can thus be written eliminating all static forces  
192 with reference to the relative position  $s = x - y$  of the mass in a frame of  
193 reference moving with the basement:

$$m\ddot{s} + c\dot{s} + Ks = -m\ddot{y} \quad (13)$$

194 which becomes the well-known second order ordinary differential equation  
195 for an oscillating body:

$$\ddot{s} + 2\beta\omega_n\dot{s} + \omega_n^2s = -\ddot{y} \quad (14)$$

196 with the introduction of the natural frequency of the oscillator:

$$\omega_n = \sqrt{K/m} \quad (15)$$

197 and of the damping ratio:

$$\beta = \frac{c}{2\sqrt{Km}} = \frac{c}{2m\omega_n} \quad (16)$$

### 198 2.3.2. *Electromagnetic damping*

199 A further important consideration is related to the damping coefficient,  
200 which can be written as:

$$c = \frac{1}{R} \left[ \frac{e(t)}{\dot{s}(t)} \right]^2 \quad (17)$$



201  $e(t)$  being the voltage generated according to Faraday's law ( $e = -d\Phi/dt$ ),  
202 and  $R$  representing the external impedance; it is assumed that inductive  
203 impedance is negligible with respect to resistive impedance in the range of  
204 frequencies here considered [8].

205 In our case, there are three coils on the oscillating mass (fig. 2), each one  
206 generating a magnetic flux that can be seen, with a good degree of accuracy,  
207 as a sinusoidal function of relative position  $s$  [12]:

$$\Phi_1(s) = \Phi_p \cos\left(\frac{2\pi}{w_t} s(t)\right) \quad (18)$$

208

$$\begin{aligned} \Phi_2(s) &= -\Phi_p \cos\left(\frac{2\pi}{w_t} \left(s(t) + \frac{1}{6} w_t\right)\right) \\ &= \Phi_p \cos\left(\frac{2\pi}{w_t} \left(s(t) + \frac{2}{3} w_t\right)\right) \end{aligned} \quad (19)$$

209

$$\Phi_3(s) = \Phi_p \cos\left(\frac{2\pi}{w_t} \left(s(t) + \frac{2}{6} w_t\right)\right) \quad (20)$$

210 where  $\Phi_p$  is the maximum value of the flux and  $w_t$  is the distance between  
211 the teeth on the stator (the second coil has opposite polarity with respect to  
212 the other coils, hence the minus sign).

213 From the time derivatives of each flux, we obtain the corresponding damp-  
214 ing coefficients:

$$c_1(t) = \frac{1}{R} \left[ \frac{2\pi\Phi_p}{w_t} \sin\left(\frac{2\pi}{w_t} s(t)\right) \right]^2 \quad (21)$$

215

$$c_2(t) = \frac{1}{R} \left[ \frac{2\pi\Phi_p}{w_t} \sin\left(\frac{2\pi}{w_t} \left(s(t) + \frac{2}{3} w_t\right)\right) \right]^2 \quad (22)$$

216

$$c_3(t) = \frac{1}{R} \left[ \frac{2\pi\Phi_p}{w_t} \sin\left(\frac{2\pi}{w_t} \left(s(t) + \frac{2}{6} w_t\right)\right) \right]^2 \quad (23)$$

217 The total force exerted is given by the sum of the forces generated by  
218 each coil, so that the overall damping coefficient is the sum of each coil's  
219 damping coefficient: since each  $c_j$  has the same sinusoidal pattern, only with  
220 a phase lag of  $w_t/6$ , the sum is a constant:

$$c(t) = \sum_{j=1}^3 c_j(t) = \frac{3}{2} \left(\frac{2\pi}{w_t}\right)^2 \frac{\Phi_p^2}{R} \quad (24)$$

221 This reasoning shows that representing the electromagnetic force with  
222 a linear dependency on velocity  $\dot{s}$  is indeed a good approximation, as long  
223 as the magnetic flux can be represented accurately enough as a sinusoidal  
224 function of relative position  $s$ .

### 225 2.3.3. Power generation

226 The steady-state response of the linear mechanical system to a harmonic  
227 forcing is itself harmonic, with an amplitude  $s_0$  given by:

$$\frac{s_0}{y_0} = \text{RAO}_s(\beta, \omega_n, \omega_e) = \frac{n^2}{\sqrt{(1-n^2)^2 + (2\beta n)^2}} \quad (25)$$

228 where  $n$  is the ratio of forcing to natural frequency:

$$n = \omega_e / \omega_n \quad (26)$$

229 In this model, electromagnetic damping provides the mean to extract  
230 energy from the wave excitation; thus, it is interesting to identify optimal  
231 values for the damping coefficient  $c$  in order to extract the maximum power.  
232 The power absorbed is given by:

$$P(t) = c\dot{s}^2 \quad (27)$$

233 and its average value over one cycle (which will be indicated as  $\Pi$ ) is:

$$\Pi = \frac{1}{T} \int_0^T P(t) dt = \frac{1}{2} c \omega_e^2 s_0^2 \quad (28)$$

234 This equation, taking into account eqs. (16) and (25), becomes:

$$\Pi = m\omega_e^3 y_0^2 \frac{n^3 \beta}{(1-n^2)^2 + (2\beta n)^2} \quad (29)$$

235 Since the oscillations are constrained by the size of the generator, two  
236 different scenarios must be considered. In the first one, let us imagine that  
237 the undamped oscillations do not reach the maximum range allowed  $s_{\max}$ :  
238 in this case, increasing the damping coefficient from 0 initially yields higher  
239 values of  $\Pi$  even though  $s_0$  decreases according to eq. (25), until a maximum  
240 for  $\Pi$  is reached, beyond which it decreases. The optimum value of  $\beta$  can  
241 thus be found when  $d\Pi/d\beta = 0$ :

$$\beta_{\text{opt}} = \frac{1}{2} \frac{|1-n^2|}{n} \quad (30)$$

242 with corresponding optimum damping coefficient, maximum average power  
243 and oscillation amplitude given by the following equations:

$$c_{\text{opt}} = m\omega_e \left| 1 - \frac{1}{n^2} \right| \quad (31)$$

244

$$\Pi_{\text{max}} = \frac{1}{4} m\omega_e^3 y_0^2 \left| 1 - \frac{1}{n^2} \right|^{-1} \quad (32)$$

245

$$s_0 = y_0 \frac{1}{\sqrt{2}} \left| 1 - \frac{1}{n^2} \right|^{-1} \quad (33)$$

246 In the second case, the undamped oscillations would be larger than the  
247 maximum allowed range  $s_{\text{max}}$ : then it is possible to extract more power by in-  
248 creasing the damping coefficient while the oscillation amplitude  $s_0$  remains at  
249 its maximum permissible level  $s_{\text{max}}$ . It is possible to show that the maximum  
250 power is obtained when the damping coefficient is such that the oscillation  
251 given by eq. (25) is exactly equal to the maximum stroke ( $s_0 = s_{\text{max}}$ ):

$$\beta_{\text{opt}} = \frac{n}{2} \sqrt{\left( \frac{y_0}{s_{\text{max}}} \right)^2 - \left( 1 - \frac{1}{n^2} \right)^2} \quad (34)$$

252

$$c_{\text{opt}} = m\omega_e \sqrt{\left( \frac{y_0}{s_{\text{max}}} \right)^2 - \left( 1 - \frac{1}{n^2} \right)^2} \quad (35)$$

253 and the corresponding maximum average power is:

$$\Pi_{\text{max}} = \frac{1}{2} m\omega_e^3 s_{\text{max}}^2 \sqrt{\left( \frac{y_0}{s_{\text{max}}} \right)^2 - \left( 1 - \frac{1}{n^2} \right)^2} \quad (36)$$

254 If the mechanical system is “tuned” to the forcing wave excitation ( $n \cong 1$ ),  
255 then the above expression can be simplified as follows:

$$\Pi_{\text{max}} \cong \frac{1}{2} m\omega_e^3 s_{\text{max}} y_0 \quad (37)$$

256 It is possible to find out which wave excitations make the system reach its  
257 maximum stroke  $s_{\text{max}}$  by setting the oscillation amplitude given by eq. (33)  
258 equal to  $s_{\text{max}}$ , yielding:

$$\frac{y_0}{s_{\text{max}}} = \sqrt{2} \left| 1 - \frac{1}{n^2} \right| \quad (38)$$

259 Thus, for wave amplitudes originating boat oscillations lower than the  
260 limit set by the above equation, the system oscillates “freely” and eqs. (31-  
261 33) apply, while for higher waves more damping, and thus more power, is  
262 available, in order to constrain the system within the maximum stroke al-  
263 lowed, and eqs. (35-36) apply.

264 It is worth to point out that in both cases the optimum value for the  
265 damping coefficient is directly proportional to the oscillator’s mass and to  
266 the forcing frequency: the average power absorbed is therefore proportional  
267 to the mass  $m$  and to the third power of forcing frequency ( $\omega^3$ ), as shown by  
268 eqs. (32) and (36).

269 In particular, the linear dependence on the oscillating mass  $m$  is, on the  
270 one hand, almost obvious because energy recovery depends on inertia and  
271 kinetic energy, but on the other hand it is an important property to be taken  
272 into account because it allows to design, test and prototype modular systems  
273 of relatively low mass, with the overall power extracted given by the sum of  
274 power available from different modules. For this reason, the results discussed  
275 in section 3 will be given with reference to a unit mass  $m = 1$  kg.

276 The frequency response of the harmonic oscillator can also be used when  
277 the external forcing is not harmonic (as in the case of a real wave excitation):  
278 if  $S_y(\omega)$  is the spectral density associated to the vertical oscillations of a  
279 particular point of interest, which can be evaluated from the wave spectral  
280 density by means of eq. (12), then the spectral density associated to the  
281 relative motion  $s$  of a linear system such as the one described in the previous  
282 section is given by:

$$S_s(\beta, \omega_n, \omega_e) = \text{RAO}_s(\beta, \omega_n, \omega_e)^2 S_y(\omega_e) \quad (39)$$

283 In the following considerations the dependence of relative motion and  
284 its spectrum on natural frequency  $\omega_n$  will be implicitly assumed, so that  
285  $S_s(\beta, \omega_e) \equiv S_s(\beta, \omega_n, \omega_e)$ .

286 The spectrum of relative motion allows the evaluation of the *significant*  
287 *oscillation amplitude* as follows:

$$s_{0s}(\beta) = 2\sqrt{m_{0s}} = 2\sqrt{\int_0^\infty S_s(\beta, \omega_e) d\omega_e} \quad (40)$$

288 Since power generation depends on the square of the generator’s velocity  
289 (eq. 27), the spectral density of relative velocity  $\dot{s}$  must be introduced. This

290 is simply given by:

$$S_{\dot{s}}(\beta, \omega_e) = \omega_e^2 S_s(\beta, \omega_e) = \omega_e^2 \text{RAO}_s(\beta, \omega_e)^2 S_y(\omega_e) \quad (41)$$

291 The zero-th momentum of the velocity spectrum gives velocity's root  
292 mean square (RMS), which is related to the average power generation:

$$\dot{s}_{\text{RMS}}(\beta) = \sqrt{m_{0\dot{s}}} = \sqrt{\int_0^\infty S_{\dot{s}}(\beta, \omega_e) d\omega_e} \quad (42)$$

293

$$\Pi_{\text{RMS}}(\beta) = \frac{c}{m} \dot{s}_{\text{RMS}}^2(\beta) = 2\beta\omega_n \dot{s}_{\text{RMS}}^2(\beta) \quad (43)$$

294 As in the case of sinusoidal waves, for a given natural frequency the  
295 generator's motion depends on the choice of the damping coefficient  $\beta$ , for  
296 which an optimum value is found by maximizing power output (eq. 43) with  
297 the constraint that the significant oscillation amplitude be lower than the  
298 maximum allowed range  $s_{\text{max}}$  (for this non-linear optimization procedure the  
299 MATLAB<sup>®</sup> function `fmincon` has been used):

$$\left. \frac{d\Pi_{\text{RMS}}}{d\beta} \right|_{\beta_{\text{opt}}} = 0 \quad \text{with} \quad s_{0s}(\beta_{\text{opt}}) \leq s_{\text{max}} \quad (44)$$

300 It must be observed that this optimization procedure is based on a sta-  
301 tistical evaluation of the oscillation amplitude, and therefore the results are  
302 approximated, because the spectrum calculated in this way contains also os-  
303 cillations higher than the constraint  $s_{\text{max}}$ : as a consequence, the actual power  
304 generation corresponding to this spectrum is somewhat lower than the value  
305 given by eq. 43 because a fraction of the energy contained in the largest  
306 oscillations is lost as the moving mass hits the shock absorbers. This pro-  
307 cess is highly non-linear, and this is the reason why it is not included in the  
308 linearised frequency-domain model here presented.

### 309 3. Results

#### 310 3.1. Yacht response

311 The foundation of the commercial software package Seakeeper, which was  
312 used to carry out the computation of the yacht's motions under different  
313 wave conditions, is the linear strip theory [21], which is used to calculate the

314 coupled heave and pitch response of the vessel; the roll response is calculated  
315 using linear roll damping theory [22].

316 The main purpose of the kinematic model presented is to provide reason-  
317 able data about the response of a generic yacht to different sea conditions, in  
318 order to have reliable information on the motion which the SEAKERS device  
319 is subjected to. Since the project does not address a particular yacht model,  
320 nor even a specific size of boat, there was no point in developing a focused  
321 in-house software: hence the choice of adopting a commercial software that  
322 has a proven record of reliability, using it to simulate the response of a yacht  
323 of adequate length included in the extensive library provided.

324 The yacht's model used in the numerical simulations is one of the library  
325 models that can be found in Seakeeper's library, since it has geometric and  
326 mass properties comparable to those of commercial sail yachts of interest for  
327 the SEAKERS project.

328 The most relevant hydrostatic properties [16] of this yacht are given in  
329 table 2, while the shape of the hull (with the indication of the waterline)  
330 and the generator's position are represented in figs. 3 and 4. The generator  
331 considered in the simulations presented is placed astern on the longitudinal  
332 axis ( $B = 0$ ) at a distance  $L = -4.20$  m from the center of gravity, i.e. close  
333 to the helm.

334 Sectional hydrodynamic masses, damping coefficients, and all other data  
335 needed in the context of the strip theory [22] have been evaluated by means  
336 of 21 two-dimensional sections (conformal mappings) approximating hull's  
337 geometry and features.

338 As illustrated in section 2.2, the yacht's response is defined by means of  
339 Response Amplitude Operators (RAO) and phase shifts, which have been  
340 obtained by means of the Seakeeper software, and provide the basis for the  
341 evaluation of the response at a particular point on the ship (eqs. 10 and 11).  
342 Figure 5 shows values of RAO at the location of the linear generator for three  
343 different speeds ( $V = [3, 6, 9]$  knt) and two headings ( $\mu = [90, 135]$  deg).

344 The response to random waves is illustrated in figs. 6 and 7 in terms  
345 of spectral density of the vertical oscillations, as defined by eq. (12). The  
346 significant oscillation amplitudes are obtained from these spectra in the same  
347 way as the significant wave amplitude is calculated from the wave spectrum  
348 [17]:

$$y_{0s} = 2\sqrt{m_{0y}} = 2\sqrt{\int_0^\infty S_y(\omega_e) d\omega_e} \quad (45)$$

349 Values of significant vertical oscillation amplitudes, corresponding to the  
350 spectral densities of figs. 6 and 7, are given in table 3.

### 351 3.2. Linear generator

352 In this section, results obtained with the mechanical model of the linear  
353 generator subject to random wave excitations, for the same conditions of  
354 speed and heading considered in section 3.1, are discussed.

355 Figures 8 and 9 show the energy spectra associated to the generator's  
356 relative motion and RMS power generation for different speeds and direc-  
357 tions. Power generation values are also given in table 4, while table 5 reports  
358 significant oscillation amplitudes.

359 The main target for the SEAKERS project is a sail yacht of length ranging  
360 from 10 to 14 m, and in this class of yachts the maximum height available  
361 for a possible installation of the device is just above 1 m: therefore, the  
362 maximum stroke taken into consideration in the simulations is  $s_{\max} = 0.5$  m.  
363 The natural frequency  $\omega_n$  is taken as 0.40 Hz, in order to make the mechanical  
364 system almost resonant with most sea conditions that may be encountered (a  
365 parametric analysis has been carried out in order to find an optimum value).

366 From table 5 it is possible to see that the generator's oscillation is almost  
367 always limited to the maximum range  $s_{\max}$ , even when the vertical oscillation  
368 of the yacht is low (table 3): this happens thanks to almost-resonant oper-  
369 ating conditions and to variable damping coefficients. In order to analyse  
370 the results, it is thus useful to consider the simplified equation for average  
371 power generation, eq. (37), which shows that, if the mechanical system is  
372 "tuned" to the forcing wave ( $n \cong 1$ ), the average power is proportional to  
373 the third power of the encounter frequency, and to the product of boat's  
374 vertical oscillation  $y_0$  and maximum range  $s_{\max}$ .

375 The spectral densities represented in figs. 8 and 9 may seem surprising at  
376 first, because the energy content appears to be almost the same for different  
377 wave heights, even though the corresponding vertical motions of the yacht  
378 are quite different (figs. 6-7 and table 3). Obviously, this just reflects the  
379 constraints on the oscillator's vertical motion, limited to  $\pm s_{\max}$ , but it does  
380 not mean that power generation is the same for different forcing conditions:  
381 as tables 4 and 6 show, more power is available with higher waves because  
382 a higher damping coefficient can be used. This underscores the relevance of  
383 a properly configured control system, able to identify ongoing sea conditions  
384 and adjust the electromagnetic properties of the system accordingly.

385 More specifically, an increase in significant wave height gives rise to two  
386 opposite effects on power generation: on the one hand it increases due to its  
387 dependence on  $y_0$ , but on the other hand the spectral density shifts towards  
388 lower frequencies (fig. 1), resulting in a decrease in power generation. Clearly,  
389 this gives rise to a maximum power generation for a particular sea state,  
390 that under the assumptions taken into account in this paper correspond to  
391 a significant wave height of 1.5 m, as figs. 8 and 9, along with table 4, show.

392 In other words, even with high values of significant wave height, which  
393 correspond to rather low values of peak frequencies (table 1), if the full  
394 spectrum is taken into account significant contributions to the excitation can  
395 be found also at relatively high frequencies, and these contributions increase  
396 average velocities and, consequently, power generation. Nonetheless, it is still  
397 possible to find that waves higher than a certain threshold actually decrease  
398 power output, because in this case significant contributions would indeed be  
399 found only at low frequencies: that is why power generation is found to be  
400 lower for 2.0 m wave height than for 1.5 m.

401 Tables 6 and 7 report values of optimum damping coefficients and damp-  
402 ing ratios as defined by the optimization procedure, eq. (44).

#### 403 4. Discussion and conclusions

404 This paper has provided an overview of the results obtained with the  
405 kinematic and mechanical models of the yacht's response to different wave  
406 excitations, and of the linear generator taken as a simple mechanical linear  
407 system which extracts power from the wave-induced motion by means of an  
408 ideal linear electromagnetic damping.

409 These preliminary evaluations, even though based on a rather simplified  
410 model of the generator, have produced some important insights on system  
411 dynamics and on the range of values to be assigned to several significant  
412 parameters, such as mechanical stiffness and damping ratio.

413 In particular, given the particular range of forcing frequencies, the me-  
414 chanical stiffness must be chosen so as to obtain a natural frequency within  
415 the range of most forcing frequencies: a value of 0.40 Hz has been considered  
416 in this paper, with a resulting stiffness-to-mass ratio around 6.3 N/(m kg).

417 The choice of damping ratios is based on the maximisation of power  
418 output for a given natural frequency for different wave excitation conditions.  
419 Values of optimum damping coefficients relative to mass have been found in



420 the range 1.3-3.9 N s/(m kg), and this result will be useful in the definition  
421 of the electric circuit's physical parameters.

422 Power generation of up to 2.1 W/kg has been obtained in the most favourable  
423 sea conditions, and anyway values higher than 0.5 W/kg are available in most  
424 cases, which represent an interesting result for this particular application.  
425 Indeed, a total weight for the SEAKERS device of up to 200 kg can be con-  
426 sidered acceptable on sail yachts with length in the range 12-14 m, especially  
427 in the case of a first equipment (as opposed to retrofitting an already ex-  
428 isting yacht, because in this case many more design constraints should be  
429 addressed). With an optimized design, it is conceivable from preliminary  
430 evaluations that up to 50% of this weight (100 kg) could be allocated to  
431 the oscillating masses; in this case, an average power generation of almost  
432 100 W is feasible, which could make possible to recover at least 1 kWh at the  
433 end of a day-long cruise. This amount of energy generation could indeed be  
434 interesting for this particular application.

435 Obviously, the issue related to the influence of this moving mass on sailing  
436 performance should be addressed: but specific calculations, which have not  
437 been reported here for brevity's sake, show that the inertial forces generated  
438 by the mass' motion are at least two orders of magnitude lower than the forces  
439 exerted by the sea on the boat. After all, this must be the case because the  
440 energy absorbed by the linear system is but a small fraction of the total  
441 energy of the incoming waves. Therefore, in all probability the impact of  
442 the added mass due to the generator on sailing performance can be safely  
443 deemed negligible.

444 It should be observed that the concept of "power availability" (or "avail-  
445 ability factor") routinely used to appreciate the performance of a system  
446 based on renewable energy, is much less useful for this particular application,  
447 because the final goal is not the generation of electricity *per se* on a continu-  
448 ous basis but, rather, only on the particular occasion when the yacht is used  
449 for a cruise. An availability factor should therefore be considered only with  
450 reference to a single cruise, and it would take into account the time frequency  
451 of encountered wave height during a typical cruise of a sailing boat, because  
452 this is the main parameter influencing average power output. However, it is  
453 rather difficult to make any prediction about this probability, other than say-  
454 ing that sail cruises are most common when wind (and, consequently, wave)  
455 conditions are not extreme (i.e. with moderate winds and waves, while it is  
456 safe to assume that calm or stormy seas are avoided); furthermore, a leisure  
457 cruise usually requires stable weather conditions. In the end, it is reasonable

458 to infer that in most cases sea conditions encountered on a leisure cruise are  
459 reasonably constant and marked by a significant wave height within the range  
460 0.5-1.5 m. Under these assumptions, average power generation is expected to  
461 be almost constant during the whole cruise.

## 462 **Acknowledgments**

463 The research leading to these results has received funding from the Eu-  
464 ropean Union Seventh Framework Programme (FP7/2007-2011) under grant  
465 agreement n. 262591. The authors would also like to acknowledge the invaluable  
466 effort provided by all the staff of Labor srl, the projects' coordinator,  
467 as well as the contribution of the SMEs and RTD performers involved in the  
468 project.

## 469 **References**

- 470 [1] de O. Falcão A. Wave energy utilization: A review of the technologies.  
471 *Renewable and Sustainable Energy Reviews* 2010;14:899–918.
- 472 [2] Langhamer O, Haikonen K, Sundberg J. Wave power—sustainable en-  
473 ergy or environmentally costly? A review with special emphasis on lin-  
474 ear wave energy converters. *Renewable and Sustainable Energy Reviews*  
475 2010;14:1329–35.
- 476 [3] Elwood D, Yim S, Prudell J, Stillinger C, von Jouanne A, Brekken T,  
477 et al. Design, construction, and ocean testing of a taut-moored dual-  
478 body wave energy converter with a linear generator power take-off. *Re-  
479 newable Energy* 2010;35:348–54.
- 480 [4] Huang SR, Chen HT, Chung CH, Chu CY, Li GC, Wu CC. Multi-  
481 variable direct-drive linear generators for wave energy. *Applied Energy*  
482 2012;100:112–7.
- 483 [5] Babarit A, Hals J, Muliawan M, Kurniawan A, Moan T, Krokstad J.  
484 Numerical benchmarking study of a selection of wave energy converters.  
485 *Renewable Energy* 2012;41:44–63.
- 486 [6] Ahn K, Truong D, Tien H, Yoon J. An innovative design of wave energy  
487 converter. *Renewable Energy* 2012;42:186–94.

- 488 [7] Stephen N. On energy harvesting from ambient vibration. *Journal of*  
489 *Sound and Vibration* 2006;293:409–25.
- 490 [8] El-hami M, Glynne-Jones P, White N, Hill M, Beeby S, James E, et al.  
491 Design and fabrication of a new vibration-based electromechanical power  
492 generator. *Sensors and Actuators* 2001;92:335–42.
- 493 [9] Ivanova I, Bernhoff H, Ågren O, Leijon M. Simulated generator for wave  
494 energy extraction in deep water. *Ocean Engineering* 2005;32:1664–78.
- 495 [10] Eriksson M, Isberg J, Leijon M. Hydrodynamic modelling of a direct  
496 drive wave energy converter. *International Journal of Engineering Sci-*  
497 *ence* 2005;43:1377–87.
- 498 [11] Leijon M, Danielsson O, Eriksson M, Thorburn K, Bernhoff H, Isberg  
499 J, et al. An electrical approach to wave energy conversion. *Renewable*  
500 *Energy* 2006;31:1309–19.
- 501 [12] Thorburn K, Leijon M. Farm size comparison with analytical model  
502 of linear generator wave energy converters. *Ocean Engineering*  
503 2007;34:908–16.
- 504 [13] Castellucci V, Waters R, Eriksson M, Leijon M. Tidal effect compen-  
505 sation system for point absorbing wave energy converters. *Renewable*  
506 *Energy* 2013;51:247–54.
- 507 [14] Beeby S, Tudor M, White N. Energy harvesting vibration sources  
508 for microsystems applications. *Measurement Science and Technology*  
509 2005;17:175–95.
- 510 [15] Bertram V. *Practical ship hydrodynamics*. Oxford, UK: Butterworth-  
511 Heinemann; 1999.
- 512 [16] Biran A. *Ship hydrostatics and stability*. Oxford, UK: Butterworth-  
513 Heinemann; 2003.
- 514 [17] Jensen J. *Load and global response of ships*. Oxford, UK: Elsevier;  
515 2001.
- 516 [18] Rawson K, Tupper E. *Basic ship theory*. Oxford, UK: Butterworth-  
517 Heinemann; 2001.

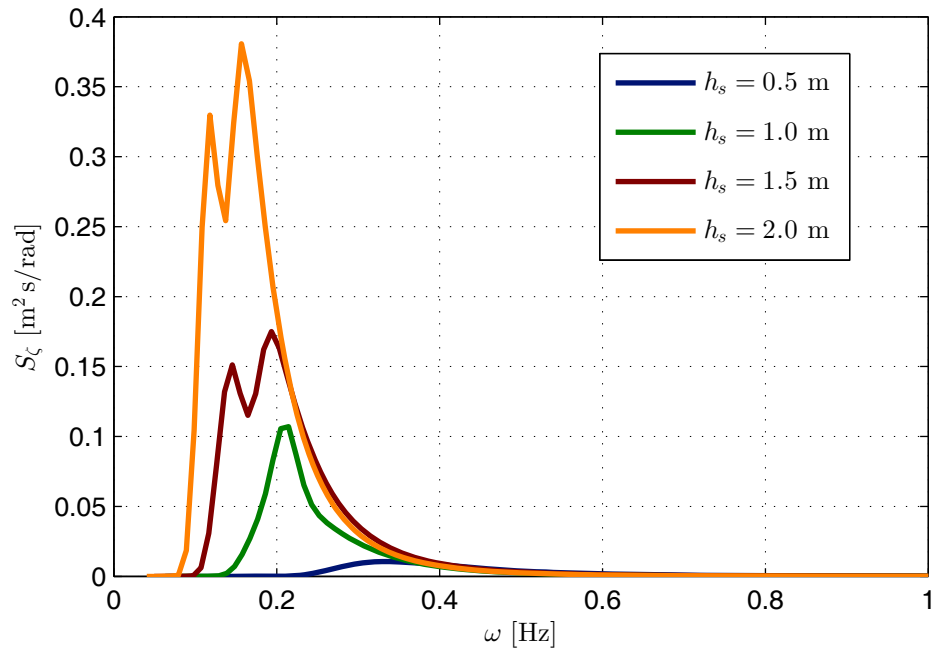
- 518 [19] Soares CG. Representation of double-peaked sea wave spectra. *Ocean*  
519 *Engineering* 1984;11:185–207.
- 520 [20] Arena F, Soares CG. Nonlinear high wave groups in bimodal sea  
521 states. *Journal of Waterway, Port, Coastal, and Ocean Engineering*  
522 2009;135:69–79.
- 523 [21] Salvesen N, Tuck O, Faltinsen O. Ship motions and sea loads. *Transac-*  
524 *tions, Society of Naval Architects and Marine Engineers* 1970;78:250–87.
- 525 [22] Seakeeper v. 16 - User Manual. Formation Design Systems Pty Ltd;  
526 2011.

527 **List of Figures**

528	1	Wave spectra representing sea conditions at Capo Linaro near	
529		Civitavecchia, Italy. . . . .	22
530	2	Representation of the linear generator: the oscillating mass	
531		(on the outside) carries coils and permanent magnets. . . . .	23
532	3	Profile view of the yacht's hull. . . . .	24
533	4	Plan view of the yacht's hull. . . . .	25
534	5	Response Amplitude Operator at the location of the linear	
535		generator. . . . .	26
536	6	Spectral density of the yacht's vertical oscillation at the gen-	
537		erator's location ( $\mu = 90$ deg). . . . .	27
538	7	Spectral density of the yacht's vertical oscillation at the gen-	
539		erator's location ( $\mu = 135$ deg). . . . .	28
540	8	Spectral density of the generator's vertical oscillation and av-	
541		erage power ( $\mu = 90$ deg). . . . .	29
542	9	Spectral density of the generator's vertical oscillation and av-	
543		erage power ( $\mu = 135$ deg). . . . .	30

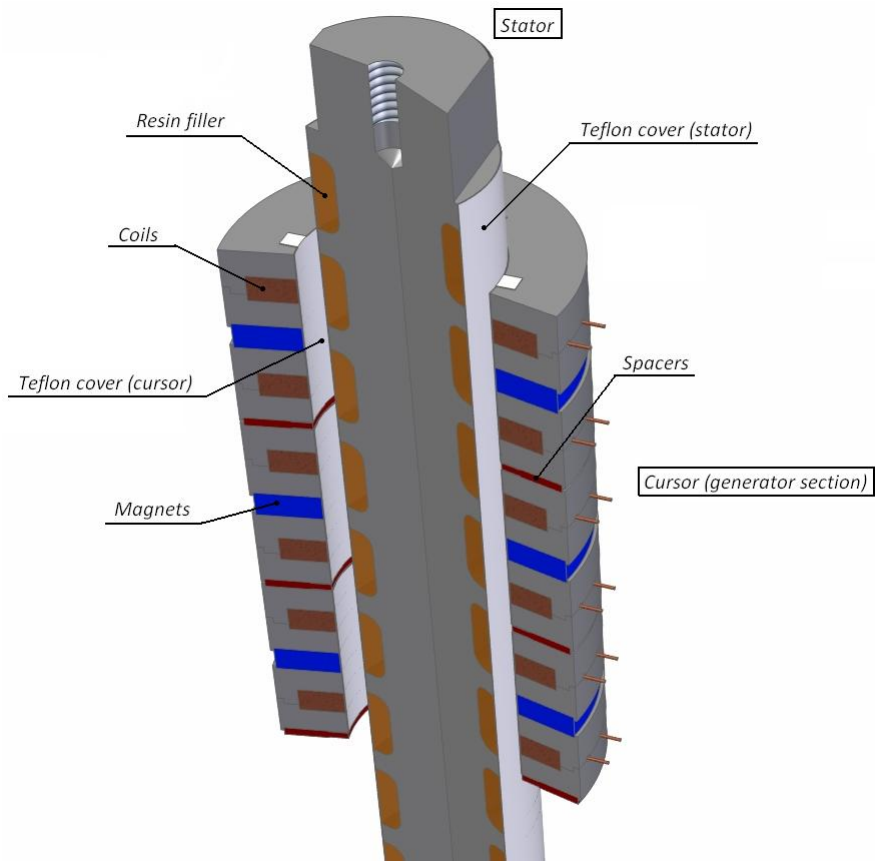
544 **List of Tables**

545	1	Parameters used to represent random sea waves at Capo Linaro	
546		near Civitavecchia, Italy. . . . .	31
547	2	Hydrostatic properties. . . . .	32
548	3	Yacht's significant vertical oscillation amplitudes at the gen-	
549		erator's location. . . . .	33
550	4	Average power generation. . . . .	34
551	5	Generator significant oscillation amplitudes. . . . .	35
552	6	Optimum damping coefficients for random wave excitation. . . . .	36
553	7	Optimum damping ratios for random wave excitation. . . . .	37



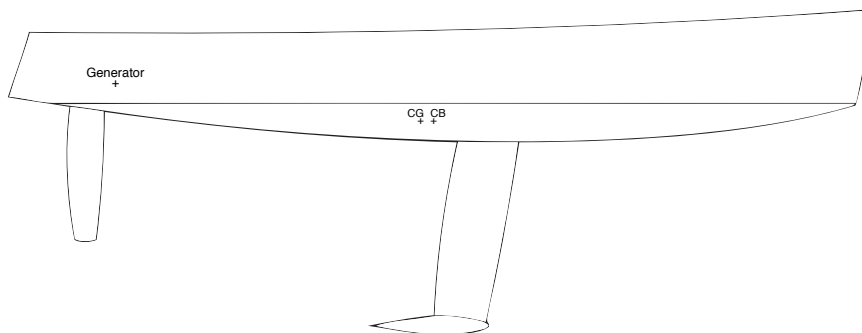
554

Figure 1: Wave spectra representing sea conditions at Capo Linaro near Civitavecchia, Italy.



555

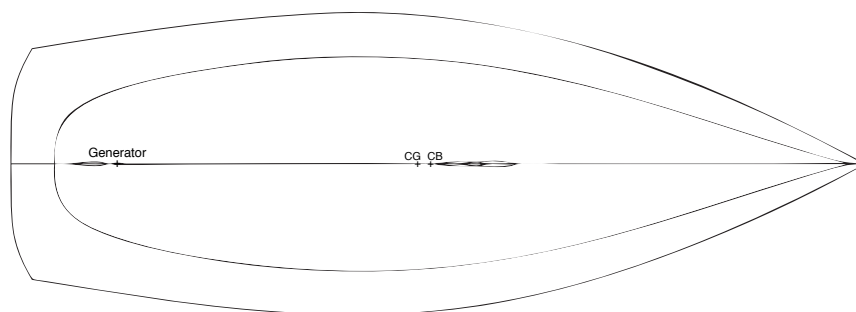
Figure 2: Representation of the linear generator: the oscillating mass (on the outside) carries coils and permanent magnets.



556

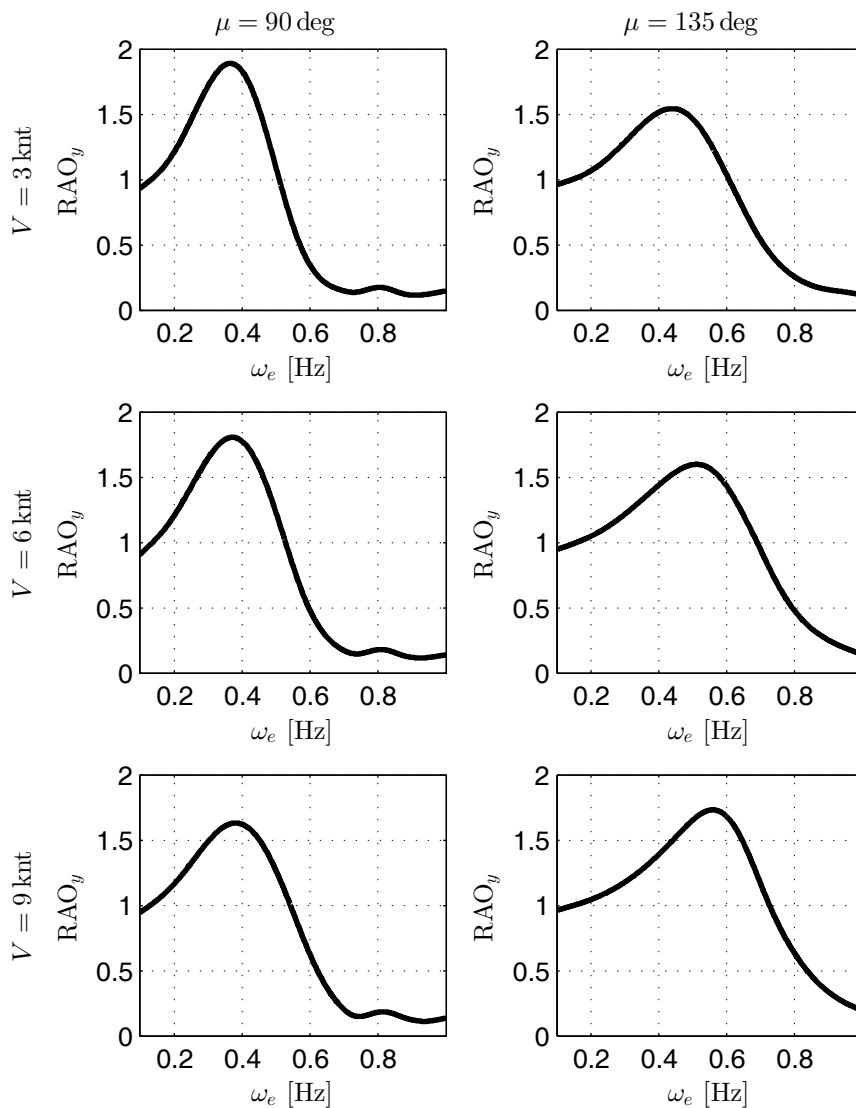
Figure 3: Profile view of the yacht's hull.





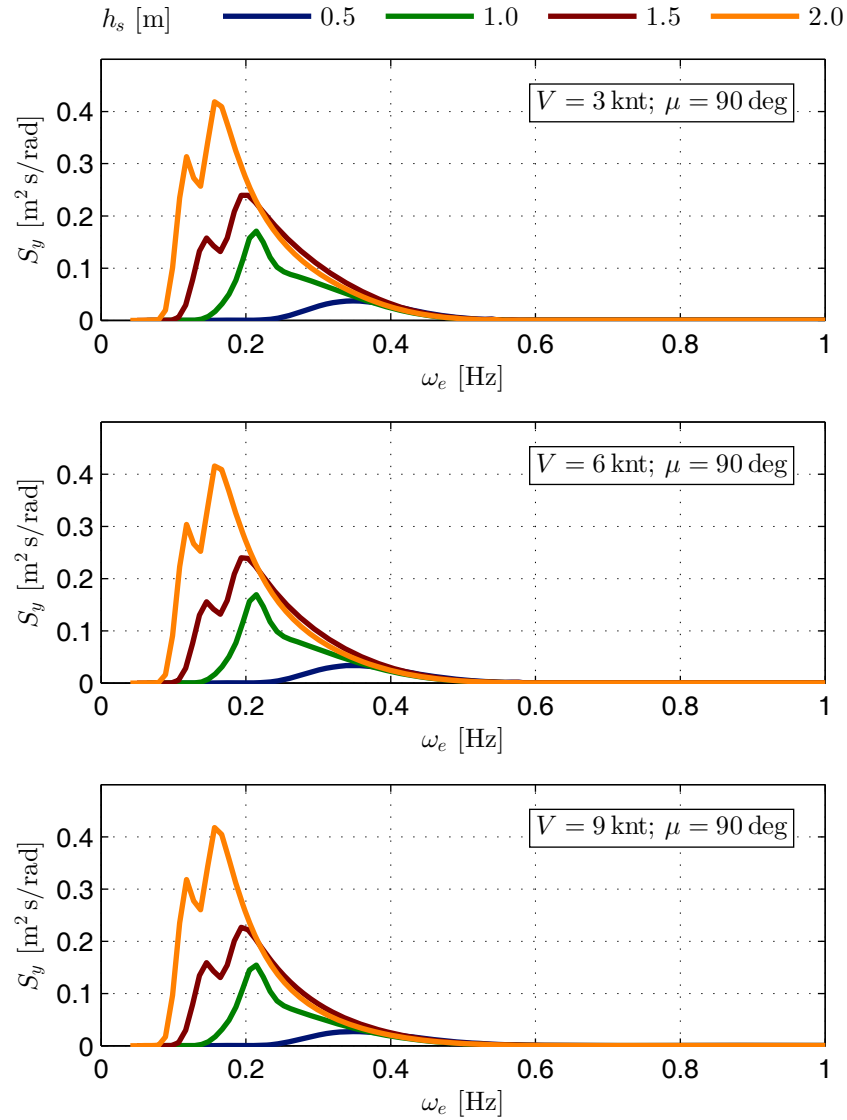
557

Figure 4: Plan view of the yacht's hull.



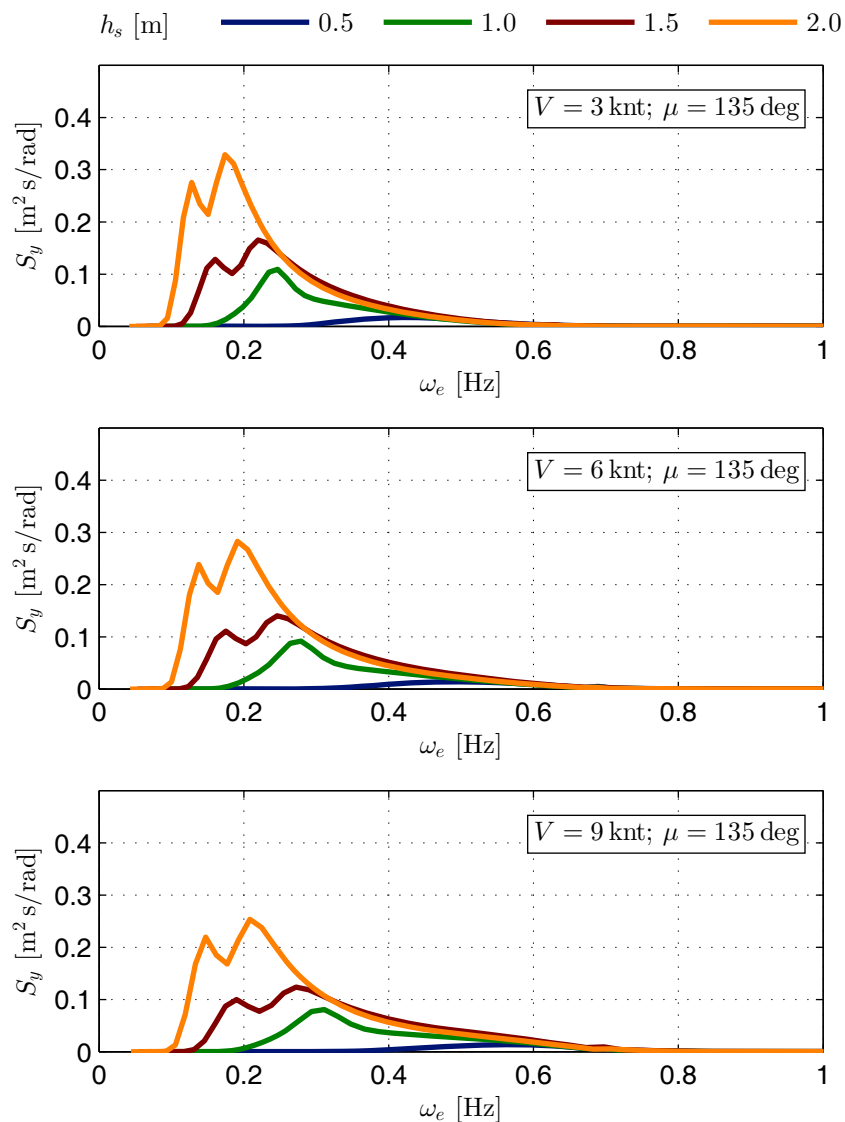
558

Figure 5: Response Amplitude Operator at the location of the linear generator.



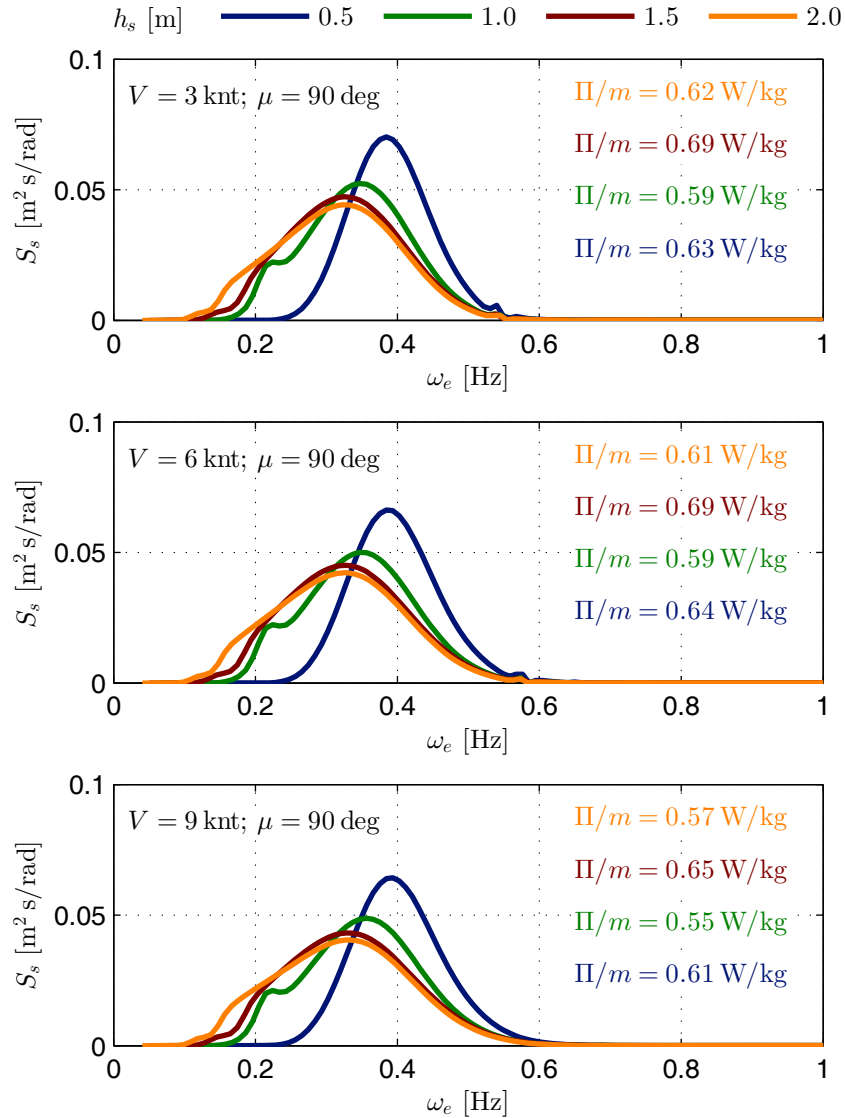
559

Figure 6: Spectral density of the yacht's vertical oscillation at the generator's location ( $\mu = 90$  deg).



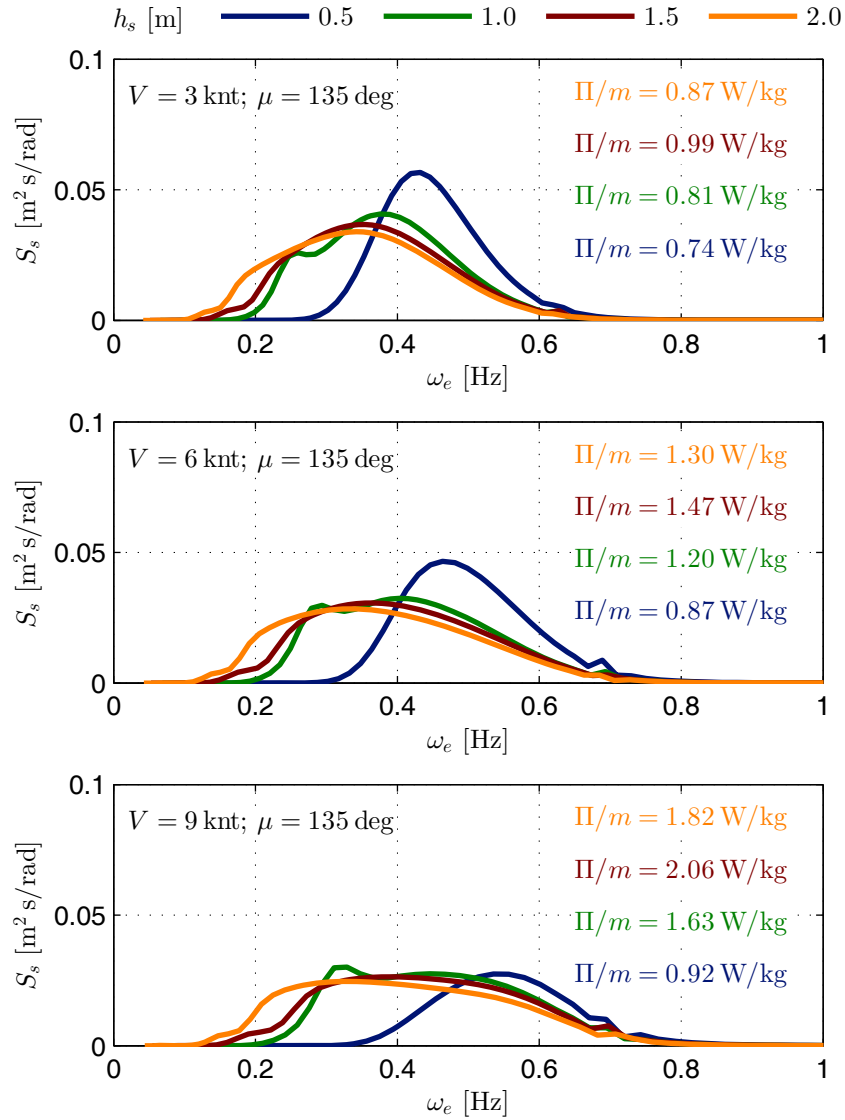
560

Figure 7: Spectral density of the yacht's vertical oscillation at the generator's location ( $\mu = 135$  deg).



561

Figure 8: Spectral density of the generator's vertical oscillation and average power ( $\mu = 90$  deg).



562

Figure 9: Spectral density of the generator's vertical oscillation and average power ( $\mu = 135$  deg).

563

$h_s$ [m]	$\alpha$	$\gamma$	$f(\alpha, \gamma)$	$T_p$ [s]
0.5	0.016	1.0	13.2	2.98
1.0	0.008	2.0	14.9	4.75
1.5	0.010	0.5	15.5	6.06
2.0	0.008	0.5	16.4	7.40

Table 1: Parameters used to represent random sea waves at Capo Linaro near Civitavecchia, Italy.

564

Property	Value
Displacement	6.531 t
Volume (displaced)	6.372 t
Overall length	11.5 m
Draft amidships	2.475 m
Immersed depth	3.054 m
Waterline length	10.64 m
Max beam on waterline	2.866 m
Max section area	1.213 m <sup>2</sup>
Waterplane area	21.21 m <sup>2</sup>
Prismatic coefficient (C <sub>p</sub> )	0.494
Block coefficient (C <sub>b</sub> )	0.068

Table 2: Hydrostatic properties.



565

$h_s$ [m]	$y_{0s}$ [m]					
	$V = 3$ knt		$V = 6$ knt		$V = 9$ knt	
	$\mu = 90^\circ$	$\mu = 135^\circ$	$\mu = 90^\circ$	$\mu = 135^\circ$	$\mu = 90^\circ$	$\mu = 135^\circ$
0.5	0.386	0.306	0.377	0.298	0.349	0.290
1.0	0.702	0.611	0.689	0.619	0.646	0.634
1.5	0.975	0.874	0.959	0.884	0.913	0.906
2.0	1.177	1.098	1.161	1.106	1.131	1.129

Table 3: Yacht's significant vertical oscillation amplitudes at the generator's location.

566

$h_s$ [m]	$\Pi_{\text{RMS}}/m$ [W/kg]					
	$V = 3$ knt		$V = 6$ knt		$V = 9$ knt	
	$\mu = 90^\circ$	$\mu = 135^\circ$	$\mu = 90^\circ$	$\mu = 135^\circ$	$\mu = 90^\circ$	$\mu = 135^\circ$
0.5	0.631	0.744	0.642	0.874	0.609	0.920
1.0	0.588	0.815	0.586	1.197	0.546	1.629
1.5	0.694	0.988	0.692	1.474	0.646	2.065
2.0	0.617	0.873	0.613	1.301	0.570	1.821

Table 4: Average power generation.

567

$h_s$ [m]	$s_{0s}$ [m]					
	$V = 3$ knt		$V = 6$ knt		$V = 9$ knt	
	$\mu = 90^\circ$	$\mu = 135^\circ$	$\mu = 90^\circ$	$\mu = 135^\circ$	$\mu = 90^\circ$	$\mu = 135^\circ$
0.5	0.500	0.500	0.500	0.500	0.500	0.404
1.0	0.500	0.500	0.500	0.500	0.500	0.500
1.5	0.500	0.500	0.500	0.500	0.500	0.500
2.0	0.500	0.500	0.500	0.500	0.500	0.500

Table 5: Generator significant oscillation amplitudes.

568

$h_s$ [m]	$c/m$ [N s/(m kg)]					
	$V = 3$ knt		$V = 6$ knt		$V = 9$ knt	
	$\mu = 90^\circ$	$\mu = 135^\circ$	$\mu = 90^\circ$	$\mu = 135^\circ$	$\mu = 90^\circ$	$\mu = 135^\circ$
0.5	1.628	1.430	1.604	1.362	1.474	1.785
1.0	1.934	2.081	1.874	2.525	1.682	2.944
1.5	2.493	2.707	2.418	3.296	2.182	3.879
2.0	2.333	2.607	2.261	3.248	2.034	3.880

Table 6: Optimum damping coefficients for random wave excitation.

569

$h_s$ [m]	$\beta$					
	$V = 3$ knt		$V = 6$ knt		$V = 9$ knt	
	$\mu = 90^\circ$	$\mu = 135^\circ$	$\mu = 90^\circ$	$\mu = 135^\circ$	$\mu = 90^\circ$	$\mu = 135^\circ$
0.5	0.324	0.284	0.319	0.271	0.293	0.355
1.0	0.385	0.414	0.373	0.502	0.335	0.586
1.5	0.496	0.539	0.481	0.656	0.434	0.772
2.0	0.464	0.519	0.450	0.646	0.405	0.772

Table 7: Optimum damping ratios for random wave excitation.